Journal of Applied Mechanics and Technical Physics, Vol. 39, No. 5, 1998

PLANE PROBLEM OF ASYMMETRICAL WAVE IMPACT ON AN ELASTIC PLATE

A. A. Korobkin and T. I. Khabakhpasheva

UDC 532.58

The problem of wave impact on the edge of an elastic horizontal plate is studied within the framework of the Wagner approach using the normal-modes method. The plate is governed by the Euler beam equation with simply supported ends. The liquid is assumed to be ideal and incompressible. The problem is coupled: the elastic and hydrodynamic characteristics of the impact process and the dimension of the contact region should be found simultaneously. An algorithm that permits a detailed study of the impact on an elastic plate is proposed. The phenomenon of unlimited increase of hydrodynamic loads owing to the plate flexibility (blockage) is revealed for fairly long plates.

Introduction. We consider a plane unsteady problem of a vertical impact of the crest of a wave on the edge of an elastic horizontal plate. Korobkin [1] solved the problem in a single-mode approximation. For fairly long plates, the phenomenon of unlimited increase of hydrodynamic loads on the plate only owing to the plate flexibility was found. This phenomenon, which is called blockage, is of doubtless interest in connection with its importance for application. To treat this phenomenon in detail, it is necessary to perform calculations by a fuller model in which the high modes of free oscillations of the plate should be taken into account. The method described in [1] allows one to carry out such calculations only on modern fast computers. In the present paper, we employed the new method that is developed for a numerical study of the central wave impact on a plate in [2] and is based on the concepts of [1]. This numerical algorithm permits one to carry out PC calculations, and hence to examine in detail the role of the elastic effects of water impact.

With other conditions being equal, the duration of the impact on the edge of a plate is longer than that of the central impact [3]. This leads to the fact that the plate–liquid interaction is expressed more strikingly in the impact on its edge than on the center. These phenomena, which we shall describe below, were not found in the case of a central impact.

Formulation of the Problem. At the initial moment of time ($t' = 0$) the crest of a wave touches the edge of an elastic plate, and this edge is assumed to the origin of the Cartesian coordinate system $x'Oy'$ (Fig. 1). The velocity of the liquid particles is equal to V and is directed upward along the normal to the undeformed surface of the plate ($y' = 0$ and $0 < x' < 2L$). The dimensional variables are primed. The wavelength is assumed to be much larger than the size of the plate, and the wave profile in the vicinity of the coordinate origin can, therefore, be approximated by a parabolic contour $y' = -x'^2/(2R)$, where R is the curvature radius at the wave crest. For long waves, we have $R \gg L$. With $t' > 0$, the liquid strikes the plate. The impact stage is completed at the moment T'_*, when the plate is completely wetted.

It is required to determine the elastic deformations of the plate, the bending-stress distribution in it, and the dimension of the contact region under the same assumptions as in [2], except the flow symmetry. In addition, it is assumed that the dimension of the wetted part of the plate is described by the single function $c'(t')$, which is unknown beforehand and should be determined simultaneously with fluid-flow and beam-deflection calculations at each moment, with $c'(0) = 0$ and $c'(T'_*) = 2L$. This assumption means that

Lavrent'ev Institute of Hydrodynamics, Siberian Division, Russian Academy of Sciences, Novosibirsk 630090. Translated from Prikladnaya Mekhanika i Tekhnicheskaya Fizika, Vol. 39, No. 5, pp. 148–158, September–October, 1998. Original article submitted November 11, 1996; revision submitted January 24, 1997.

 0021-8944/98/3905-0782 $20.00

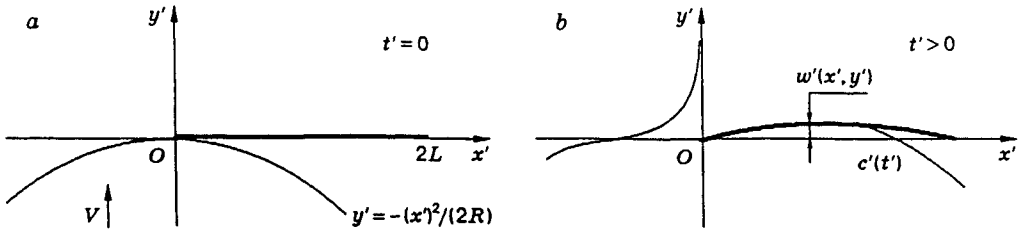

Fig. 1

the liquid adjoins to the plate in the contact region $0 < x' < c'(t')$ irrespective of the pressure in this region, i.e., cavitational phenomena are ignored.

At the initial stage of impact on the weakly curved surfaces ($\varepsilon \ll 1$), the equations that describe the flow of a liquid and the deformation of an elastic body and the boundary conditions on a free surface and in the contact region can be linearized [2]. Also, the boundary conditions can be shifted to the $y' = 0$ line. Despite the linearization, the problem, however, remains nonlinear, because one needs to determine not only the hydrodynamic and elastic characteristics but also the dimension of the contact region.

To consider the problem in dimensionless variables, we choose the same scales of variation of the variables as those in the case of a central impact [2]. All the dimensionless parameters in the formulation of the problem do not exceed unity. The notation of the dimensionless variables is primeless.

The formulation of the problem has the form

$$\alpha\frac{\partial^2 w}{\partial t^2} + \beta\frac{\partial^4 w}{\partial x^4} = p(x,0,t) \qquad (0 < x < 2,\ t > 0); \tag{1}$$

$$w = w_{xx} = 0 \quad (x = 0,\ x = 2,\ t \geqslant 0), \qquad w = w_t = 0 \quad (0 < x < 2,\ t = 0); \tag{2}$$

$$p = -\varphi_t \qquad (y \leqslant 0); \tag{3}$$

$$\varphi_{xx} + \varphi_{yy} = 0 \qquad (y < 0); \tag{4}$$

$$\varphi = 0 \quad (y = 0,\ x < 0,\ x > c(t)), \qquad \varphi_y = -1 + w_t(x,t) \quad [y = 0,\ 0 < x < c(t)]; \tag{5}$$

$$\varphi \to 0 \qquad (x^2 + y^2 \to \infty). \tag{6}$$

Here $p(x,y,t)$ is the pressure of the liquid, the function $w(x,t)$ determines the beam deflection at the point with the x coordinate at the moment t, and $\varphi(x,y,t)$ is the velocity potential. The interval of the fluid boundary $y = 0$, $0 < x < c(t)$ corresponds to the contact region, and the semi-infinite intervals $y = 0$, $x < 0$ and $y = 0$, $\sigma(x,t)$ correspond to the free surface. The distribution of the bending stresses in the beam $\sigma(x,t)$ is determined by the formula $\sigma(x,t) = zw_{xx}(x,t)/2$, where the variable z varies over the thickness of the beam ($z = -1$ corresponds to its lower wetted side, and $z = +1$ to the upper side in the largest-thickness sites). The dimensionless parameters α and β [see [2]) are equal to

$$\alpha = \frac{M_B}{\rho L}, \qquad \beta = \frac{EJ}{\rho L(RV)^2}.$$

The impact stage ends at the moment T_*, when $c(T_*) = 2$. The formulation of problem (1)–(6) should be supplemented by the equation for the function $c(t)$. This equation follows from the condition that the displacements of liquid particles in the neighborhood of the moving point of contact $x = c(t)$ are bounded and has the form [1]

$$t = \frac{5}{16}c^2 + \frac{4}{\pi}æ\int_0^{\pi/2} \sin^2\theta w[c(t)\sin^2\theta, t]\,d\theta. \tag{7}$$

Problem (1)–(7) is studied using the normal modes method, which was described in detail in [2].

Method of Normal Modes. Within the framework of this method, the beam deflection $w(x,t)$ and the velocity potential $\varphi(x,0,t)$ on the part of the liquid boundary $y = 0$, $0 < x < 2$ are found in the form of series in the eigenfunctions $\psi_n(x)$ of the problems of free oscillations of the beam with homogeneous boundary conditions for these functions and their second derivatives for $x = 0$ and $x = 2$ (see [2, formulas (13) and (14)]):

$$w(x,t) = \sum_{n=1}^{\infty} a_n(t)\psi_n(x), \qquad \varphi(x,0,t) = \sum_{n=1}^{\infty} b_n(t)\psi_n(x). \tag{8}$$

After normalization for a simply supported beam, we find that $\psi_n(x) = \sin(\lambda_n x)$ and $\lambda_n = (\pi n)/2$, where $n = 1, 2, 3, \ldots$ are eigenvalues. With allowance for (5), Eqs. (8) yield

$$b_n(t) = \int_0^{c(t)} \varphi(x,0,t)\psi_n(x)\,dx. \tag{9}$$

Substituting the representations (8) in the beam equation (1) and taking into consideration (3) and (9), for the generalized coordinates $a_n(t)$ and $b_n(t)$ we obtain the equation

$$\alpha\ddot{a}_n + \dot{b}_n + \beta\lambda_n^4 a_n = 0. \tag{10}$$

The point denotes the derivative in time. In this equation, the quantities b_n depend on the derivatives $\dot{a}_m$, where $m = 1, 2, 3, \ldots$, and on the dimension of the contact region c.

In this case, it is convenient to introduce the new harmonic functions $\varphi_n(x,y,c)$ as the solutions of the boundary-value problem

$$\frac{\partial^2\varphi_n}{\partial x^2} + \frac{\partial^2\varphi_n}{\partial y^2} = 0 \qquad (y < 0); \tag{11}$$

$$\varphi_n = 0 \quad [y = 0,\ x < 0,\ x > c(t)], \qquad \frac{\partial\varphi_n}{\partial y} = \psi_n(x) \quad [y = 0,\ 0 < x < c(t)]; \tag{12}$$

$$\varphi_n \to 0 \quad (x^2 + y^2 \to \infty) \tag{13}$$

with integrable singularities of the first derivatives near the boundary points $y = 0$ and $x = 0$ and $y = 0$ and $x = c$. Here $n = 0, 1, 2, \ldots$ and $\psi_0(x) \equiv 1$. After the boundary-value problem (11)–(13) is solved, equalities (5), (8), and (9) give

$$\varphi(x,0,t) = -\varphi_0(x,0,c) + \sum_{n=1}^{\infty} \dot{a}_n(t)\varphi_n(x,0,c), \qquad b_m(t) = -f_m(c) + \sum_{n=1}^{\infty} \dot{a}_n(t)S_{nm}(c); \tag{14}$$

$$f_m(c) = \int_0^c \varphi_0(x,0,c)\psi_m(x)\,dx; \tag{15}$$

$$S_{nm}(c) = \int_0^c \varphi_n(x,0,c)\psi_m(x)\,dx. \tag{16}$$

The added-mass matrix S with the elements $S_{nm}(c)$, $n, m = 1, 2, \ldots$ is symmetric, which follows from Green's second integral theorem.

We introduce the auxiliary vector $\mathbf{d} = (d_1, d_2, d_3, \ldots)^t$, where $d_n = (\alpha\dot{a}_n + b_n)/(\beta\lambda_n^4)$, the vectors $\mathbf{a} = (a_1, a_2, a_3, \ldots)^t$ and $\mathbf{f} = (f_1(c), f_2(c), f_3(c), \ldots)^t$, and the diagonal matrix $D = \operatorname{diag}\{\lambda_1^4, \lambda_2^4, \lambda_3^4, \ldots\}$ by means of which Eqs. (10) can be rewritten in matrix form:

$$\frac{d\mathbf{a}}{dt} = (\alpha I + S)^{-1}(\beta D\mathbf{d} + \mathbf{f}), \qquad \frac{d\mathbf{d}}{dt} = -\mathbf{a}. \tag{17}$$

The right-hand sides in (17) depend on $\mathbf{a}$, $\mathbf{d}$, and c and do not depend on the time t; therefore, it is convenient to choose the quantity c as the new independent variable, $0 \leqslant c \leqslant 2$. Here the new required

function $t = t(c)$ appears as the differential equation which follows from (7) and has the form [1]

$$\frac{dt}{dc} = Q(c, \mathrm{a}, \dot{\mathrm{a}}), \qquad Q(c, \mathrm{a}, \dot{\mathrm{a}}) = \frac{5c/8 + (\mathrm{a}, \boldsymbol{\Gamma}_c(c))}{1 - (\dot{\mathrm{a}}, \boldsymbol{\Gamma}(c))}. \tag{18}$$

The components of the vectors $\boldsymbol{\Gamma}(c)$ and $\boldsymbol{\Gamma}_c(c)$ are given by the formulas

$$\Gamma_n(c) = \frac{4}{\pi}\int_0^{\pi/2} \sin^2\theta\psi_n(c\sin\theta)\,d\theta, \qquad \Gamma_{nc}(c) = \frac{4}{\pi}\int_0^{\pi/2} \sin^4\theta\,\psi_n'(c\sin\theta)\,d\theta.$$

Multiplying each equation of system (17) by dt/dc and making allowance for (18), we find

$$\frac{d\mathrm{a}}{dc} = \mathbf{F}(c, \mathrm{d})Q(c, \mathrm{a}, \mathbf{F}(c, \mathrm{d})); \tag{19}$$

$$\frac{d\mathrm{d}}{dc} = -\mathrm{a}Q(c, \mathrm{a}, \mathbf{F}(c, \mathrm{d})), \tag{20}$$

where $\mathbf{F}(c, \mathrm{d}) = (\alpha I + æS(c))^{-1}(\beta D\mathrm{d} + \mathbf{f}(c))$. System (18)–(20) is solved numerically under the zero initial conditions

$$\mathrm{a} = 0, \qquad \mathrm{d} = 0, \qquad t = 0 \quad (c = 0). \tag{21}$$

The derivatives $\dot{a}_n(t)$ are determined by the formula $\dot{a}_n = F_n(c, \mathrm{d})$.

It is noteworthy that the form of the Cauchy problem (18)–(21) coincides with the form of the corresponding problem on the central wave impact on an elastic plate. However, the terms entering system (18)–(20) are determined by other formulas and should be investigated independently. The presented formulation of the problem remains valid under any conditions for supporting the beam ends.

The direct calculations yield

$$\begin{gathered}\Gamma_n(c) = \sin\xi J_0(\xi) + \cos\xi J_1(\xi), \qquad \xi = \frac{\lambda_n c}{2}, \\ \Gamma_{nc}(c) = \lambda_n\Big(\cos\xi J_0(\xi) - \sin\xi J_1(\xi) - \frac{1}{2\xi}\cos\xi J_1(\xi)\Big)\end{gathered} \tag{22}$$

for the case of a simply supported beam.

In a numerical solution of the Cauchy problem (18)–(21), it is necessary to invert the matrix S at each step on c, where $0 < c \leqslant 2$. Therefore, the possibility itself of the solution of the problem is mainly determined by the effectiveness of calculation of the functions $S_{nm}(c)$ and $f_m(c)$, where $m, n = 1, 2, 3, \ldots$.

Added-Mass Matrix. The functions $f_m(c)$ and $S_{nm}(c)$ are determined by formulas (15) and (16). Substituting $\psi_m(x) = \sin\lambda_m x$ in them and integrating by parts with allowance for the equalities $\varphi_n(0, 0, c) = \varphi_n(c, 0, c) = 0$, where $n = 0, 1, 2, 3, \ldots$, we obtain

$$f_m(c) = \frac{1}{\lambda_m}\int_0^c \cos(\lambda_m x)\frac{\partial\varphi_0}{\partial x}(x, 0, c)\,dx; \tag{23}$$

$$S_{nm}(c) = \frac{1}{\lambda_m}\int_0^c \cos(\lambda_m x)\frac{\partial\varphi_n}{\partial x}(x, 0, c)\,dx. \tag{24}$$

The derivatives in the last integrals equal

$$\frac{\partial\varphi_n}{\partial x}(x, 0, c) = \frac{1}{\pi\sqrt{x(c-x)}}\,\text{V.p.}\int_0^c \frac{\sqrt{\mu(c-\mu)}\,\psi_n(\mu)}{\mu - x}\,d\mu \tag{25}$$

for $0 < x < c$ [3]; in particular,

$$\frac{\partial\varphi_0}{\partial x}(x, 0, c) = \frac{c/2 - x}{\sqrt{x(c-x)}}. \tag{26}$$

Calculating the integral in (23) with allowance for (26), we have

$$f_m(c) = \frac{\pi c^2 \sin\lambda}{4\lambda} J_1(\lambda), \qquad \lambda = \frac{\lambda_m c}{2}. \tag{27}$$

The determination of the integrals (24) and (25) for $n = 1, 2, 3, \ldots$ is not trivial, and therefore we shall give it below. It is convenient to introduce the new integration variables $x = c(\xi + 1)/2$ and $\mu = c(\sigma + 1)/2$ into (24) and (25), respectively. We obtain

$$S_{nm}(c) = \frac{c^2}{4\pi\lambda} \int_{-1}^{1} \frac{\cos(\lambda\xi + \lambda)}{\sqrt{1-\xi^2}} \Big(\text{V.p.} \int_{-1}^{1} \frac{\sqrt{1-\sigma^2}\, \sin(\zeta\sigma + \zeta)}{\sigma - \xi}\, d\sigma \Big)\, d\xi,$$

where $\lambda = \lambda_m c/2$ and $\zeta = \lambda_n c/2$. Using the expansions of the sums of trigonometrical functions and the parity properties of the Hilbert transformation relative to the finite interval, we find

$$S_{nm}(c) = \frac{c^2}{4\pi\lambda} \Big[\cos\lambda \cos\zeta S^{(1)}_{nm} - \sin\lambda \sin\zeta S^{(2)}_{nm} \Big],$$

$$S^{(1)}_{nm} = \int_{-1}^{1} \frac{\cos\lambda\xi}{\sqrt{1-\xi^2}} \Big(\text{V.p.} \int_{-1}^{1} \frac{\sqrt{1-\sigma^2}\sin\zeta\sigma}{\sigma - \xi}\, d\sigma \Big)\, d\xi; \tag{28}$$

$$S^{(2)}_{nm} = \int_{-1}^{1} \frac{\sin\lambda\xi}{\sqrt{1-\xi^2}} \Big(\text{V.p.} \int_{-1}^{1} \frac{\sqrt{1-\sigma^2}\cos\zeta\sigma}{\sigma - \xi}\, d\sigma \Big)\, d\xi. \tag{29}$$

We first calculate the internal integral in (28). To do this, we use the expansion [4]

$$\sin\zeta\sigma = 2 \sum_{k=0}^{\infty} (-1)^k J_{2k+1}(\zeta) T_{2k+1}(\sigma) \quad (-1 \leqslant \sigma \leqslant 1)$$

and the orthogonality of the Chebyshev polynomials $T_n(\sigma)$. We obtain

$$\text{V.p.} \int_{-1}^{1} \frac{\sqrt{1-\sigma^2}\sin\zeta\sigma}{\sigma - \xi}\, d\sigma = -\pi J_1(\zeta) + 2\pi(1-\xi^2) \sum_{k=0}^{\infty} (-1)^k J_{2k+1}(\zeta) U_{2k}(\xi),$$

where $U_k(\xi)$ are the second-kind Chebyshev polynomials. Substitution of the last expansion in (28) with allowance for the value of the integral

$$\int_{-1}^{1} \sqrt{1-\sigma^2} U_{2k}(\xi) \cos\lambda\xi\, d\xi = \frac{2\pi}{\lambda} (-1)^k (2k+1) J_{2k+1}(\lambda)$$

gives

$$S^{(1)}_{nm} = -\pi^2 J_0(\lambda) J_1(\zeta) + \frac{2\pi^2}{\lambda} \sum_{k=0}^{\infty} (2k+1) J_{2k+1}(\zeta) J_{2k+1}(\lambda).$$

The last series is tabular [5], which allows us to write

$$S^{(1)}_{nm} = \frac{\pi^2\lambda}{\zeta^2 - \lambda^2} [\lambda J_0(\lambda) J_1(\zeta) - \zeta J_0(\zeta) J_1(\lambda)]. \tag{30}$$

In particular, for $\zeta = \lambda$ we have

$$S^{(1)}_{nn} = -\pi^2 J_0(\lambda) J_1(\lambda) + \frac{\pi^2\lambda}{2} (J_0^2(\lambda) + J_1^2(\lambda)). \tag{31}$$

The integrals in (29) are calculated similarly:

$$S^{(2)}_{nm} = \frac{\pi^2\lambda}{\zeta^2 - \lambda^2} [\lambda J_1(\lambda) J_0(\zeta) - \zeta J_1(\zeta) J_0(\lambda)]; \tag{32}$$

$$S_{nn}^{(2)} = -\frac{\pi^2\lambda}{2}(J_0^2(\lambda) + J_1^2(\lambda)). \tag{33}$$

The Bessel functions in (22), (27), and (30)–(33) are calculated with the use of their polynomial approximations [4].

Hydrodynamic Impact Force. After the solution of the Cauchy problem (18)–(21), the plate deflection is determined by formula (8), and the distribution of the bending stresses by the formula

$$\sigma(x,t) = -\frac{\pi^2}{8}\sum_{n=1}^{\infty} n^2 a_n(t)\sin\left(\frac{\pi n x}{2}\right).$$

In dimensionless variables, the force acting on the plate from the side of the liquid is determined by the integral

$$F(t) = -\int_0^{c(t)} \varphi_t(x,0,t)\,dx, \tag{34}$$

and the scale of force is equal to $\rho V^2 R$. With allowance for the continuity of the velocity potential at the liquid boundary $y = 0$, formula (34) gives

$$F(t) = -\frac{d}{dt}q(t), \qquad q(t) = \int_0^{c(t)} \varphi(x,0,t)\,dx. \tag{35}$$

In the impact stage, the function $q(t)$ can be calculated with the use of expansion (8), where $b_n(t) = \beta\lambda_n^4 d_n(t) - \alpha\dot{a}_n(t)$. This expansion can be differentiated termwise with respect to t, but the resulting series converges very slowly, and this does not allow one to perform calculations directly by formula (34). Therefore, one needs to use (35): to calculate first the function $q(t)$ and then to differentiate it numerically with respect to the time.

We determine the function $q(t)$ independently, using the method of [3]. We consider a perturbed flow of a liquid far from the contact region. As the scale of length increases, the spot of contact becomes a point, and, in the first approximation, conditions (5) at the boundary of the flow region can be replaced by the single condition [3]

$$\varphi = q(t)\delta(x) \qquad (y = 0),$$

where $\delta(x)$ is the Dirac delta-function. As $y \to -\infty$ and $x = 0$, the solution of Eq. (4) with this boundary condition gives

$$\varphi_y(0,y,t) \sim \frac{q(t)}{\pi y^2}.$$

As $y \to -\infty$, the vertical velocity component $\varphi_y(0,y,t)$ also can be determined by solving the problem relative to the displacements of the liquid particles [1]. We have

$$\varphi_y(0,y,t) \sim \frac{1}{\pi y^2}\frac{d}{dt}\int_0^{c(t)} \sqrt{\sigma(c-\sigma)}\left(\frac{1}{2}\sigma^2 - t + w(\sigma,t)\right)d\sigma.$$

Comparing the last two asymptotic formulas, we obtain

$$q(t) = -\int_0^{c(t)} \sqrt{\sigma(c-\sigma)}(1 - w_t(\sigma,t))\,d\sigma.$$

Using the representation of w in the form of series (8), we rewrite the expression for $q(t)$ as follows:

$$q(t) = \sum_{m=1}^{\infty} \dot{a}_m(t)s_m(c) - \frac{\pi}{8}c^2, \qquad s_m(c) = \int_0^c \sqrt{\sigma(c-\sigma)}\psi_m(\sigma)\,d\sigma. \tag{36}$$

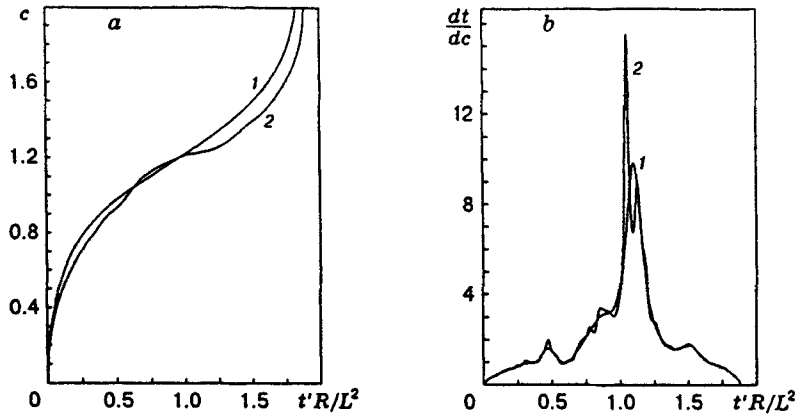

Fig. 2

In our case, $\psi_m(\sigma) = \sin \lambda_m \sigma$ and $\lambda = \pi m/2$, and hence

$$s_m(c) = \frac{c}{m} \sin\left(\frac{\pi m c}{4}\right) J_1\left(\frac{\pi m c}{4}\right).$$

It is seen that $s_m(c) = O(m^{-3/2})$ as $m \to \infty$. It was shown in [2] that $\dot{a}_m(t) = O(m^{-2})$ as $m \to \infty$, and therefore the series in (36) converges quite rapidly and can be found numerically. For an undeformable plate, when $w(x,t) \equiv 0$, Eq. (7) yields $c_R(t) = (16t/5)^{1/2}$. The quantities related to the case of a rigid plate have the subscript R. We find $q_R(t) = -(\pi/8)c_R^2(t)$ from (36), and hence $q_R(t) = -(2/5)\pi t$ and $F_R(t) = 2\pi/5$.

For small times ($t \ll 1$), the elasticity of the plate can be ignored, and therefore $F(0) = F_R(0)$. The ratio $F(t)/F_R(t)$ is specified by the formula

$$\frac{F(t)}{F_R(t)} = \frac{5}{16}\frac{d}{dt}\left\{c^2 - \frac{8}{\pi}c\sum_{n=1}^{\infty}\frac{\dot{a}_n(t)}{n}\sin\left(\frac{\pi n c}{4}\right)J_1\left(\frac{\pi n c}{4}\right)\right\} \tag{37}$$

used in calculations.

Results of a Numerical Analysis. The Cauchy problem (18)–(21) is solved numerically by the fourth-order Runge–Kutta method with a constant step relative to the variable c. The choice of the step was considered at great length in [2]. However, this approach entails difficulties at small velocities of the contact point dc/dt. In this case, small variations of c gives rise to significant changes in the function $t(c)$. For large values of the derivative dt/dc, the following procedure was applied: if $dt/dc < 3$, calculations were performed by the model (18)–(20) with the independent variable c; otherwise the time t was used as the independent variable and calculations were done with the use of the model (17) with an additional equation for $c(t)$:

$$\frac{dc}{dt} = \frac{1}{Q(c, a, \dot{a})}.$$

The time step was assumed to be equal to that relative to c. As soon as the velocity of extension of the contact region increased up to 1/3, we returned to the initial model.

The problem was solved for $\alpha = 0.157$ and $\beta = 0.04$. These values of the parameters correspond to the impact on the edge of a plate of thickness 1 cm and length 1 m and made from steel ($\rho_b = 7850$ kg/m^3, $E = 21 \cdot 10^{10}$ N/m^2) by the wave crest for which product $RV = 30$ m^2/sec (e.g., $R = 10$ m and $v = 3$ m/sec or $R = 20$ m and $v = 1.5$ m/sec). We note that the use of the model of an incompressible fluid is justified in the case where the duration of the impact stage [it is of the order of $L^2/(RV)$] exceeds considerably the duration of the acoustic stage of impact (it is of the order of $T_{ac} = RV/c_0^2$ [6], where c_0 is the sound velocity in a quiescent liquid under normal conditions). In the case considered, we have $T = 625T_{ac}$, and therefore ignoring the acoustic effects is justified.

Figure 2a shows the dependence of the size of the contact region c on the time t, calculated in the one-mode approximation (curve 1) and with allowance for the first twenty modes (curve 2). Clearly, the one-

mode approximation gives correct insight into the enlargement of the wetted part of the plate on impact. Similar curves, constructed with the use of five or more modes, practically coincide with curve 2. However, to calculate the "inverse rate of wetting" $(dt/dc)(t)$, it is necessary to use the larger number of modes, the one-mode approximation gives the incorrect rate of wetting of the plate. Figure 2b shows the dependence of dt/dc on the time, which was found with the use of the first five modes (curve 1) and of the first ten modes (curve 2). The curves are in agreement with each other outside the interval $1 < t < 1.2$. Inside this interval, the derivative dt/dc changes abruptly and takes the maximum value. For a good approximation of the inverse rate of wetting, it is necessary to take into account ten modes, because the calculations with a smaller number of modes give the underestimated values of the maximum of dt/dc. The increase in the number of modes allows one to clarify the details of variation of the rate of wetting with time, which can be considered insignificant. In particular, the maximum of the derivative dt/dc and the width of the region of abrupt changes in dt/dc, found with the use of ten modes, are almost the same. It means that the complex shape of curve 2 in Fig. 2b is not caused by the errors of the numerical calculation but reflects the irregular character of the interaction between the elastic surface and the liquid on impact.

The process of elastic-plate wetting on impact can be described as follows. In the initial stage, the rate of wetting exceeds significantly the impact velocity and decreases slowly with time until the contact region reaches the dimension $1.2L$. Here the rate of wetting exceeds 15 m/sec. Further, the rate of wetting drops sharply to 4 m/sec owing to the elastic properties of the body and becomes comparable with the impact velocity. For undeformable bodies, this effect was not observed [3]. The low rate of wetting does not occur for long, and it then increases and becomes unbounded at the end of the impact stage.

The force $F(t)$ that acts from the side of the liquid on the plate, is approximately proportional to the dimension of the contact region $c(t)$, the rate of its expansion dc/dt, and the impact velocity [see (37)]. At the initial stage, the rate of wetting is high, which explains considerable hydrodynamic loads on the plate. These loads cause the plate deflection and, in particular, a decrease in the local impact velocity $v(x,t) = 1 - w_t(x,t)$. Here the rate of wetting decreases, as a portion of the liquid follows the plate deflection, instead of the propagation along the plate. For soft plates with a small value of the parameter β, the rate of wetting can fall off substantially. To explain the drastic character of variation of this rate, we calculate the periods T_n of the eigenoscillations of the plate in a vacuum. We have $T_n = T_1/n^2$ and $T_1 = (8/\pi)(\alpha/\beta)^{1/2}$ in dimensionless variables, and hence $T_1 \approx 16$, $T_2 \approx 4$, $T_3 \approx 2$, $T_4 \approx 1$, and $T_5 \approx 2/3$. As is seen, the first three modes cannot be responsible for the details of the process, because the duration of the impact stage is less than 2. The distinguishing features of the impact process at this stage are due to higher modes, starting with the fourth mode.

The model used is valid only in the case where the rate dc/dt is positive and finite. If the rate of wetting vanishes and then becomes negative, the liquid particles from the contact region reaches the free surface, and a vortex layer, which is ignored in the present model, is formed. If the rate of wetting grows and becomes comparable with the sound velocity in the liquid, the assumption of fluid incompressibility becomes invalid and it is necessary to consider the more complicated acoustic approximation. Figure 2b shows that in the middle of the impact stage the rate of wetting falls off substantially but remains positive. Further, the rate of wetting increases unboundedly $(dt/dc \to 0)$. It is important to note that $c_* < 2$, where c_* is such that $(dt/dc)(c_*) = 0$. In this case, the model does not allow one to describe the impact stage completely; at the end of the impact stage the velocity of extension of the contact region becomes so large that acoustic effects should be included.

The force that acts on the plate from the side of the liquid is shown in Fig. 3a as a function of the dimension of the contact region c. In the calculations by formula (37), the first twenty modes were used. It is seen that the hydrodynamic loads grow infinitely as $c \to c_*$. This phenomenon is called blockage. In the blockage owing to the elastic deformations of the plate, the velocity of the contact point increases, which leads to the unbounded growth of hydrodynamic loads. The blockage was not observed in the case of a central impact, i.e., the site of impact is determining for this phenomenon.

The resisting force also varies abruptly in the section of abrupt change of the derivative $(dt/dc)(t)$ (Fig. 2b) and takes negative values (see Fig. 3a). The latter indicates the possibility of cavitational phenomena

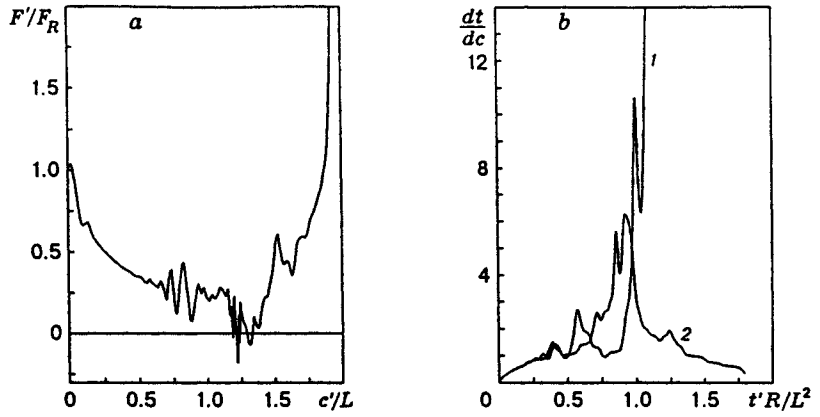

Fig. 3

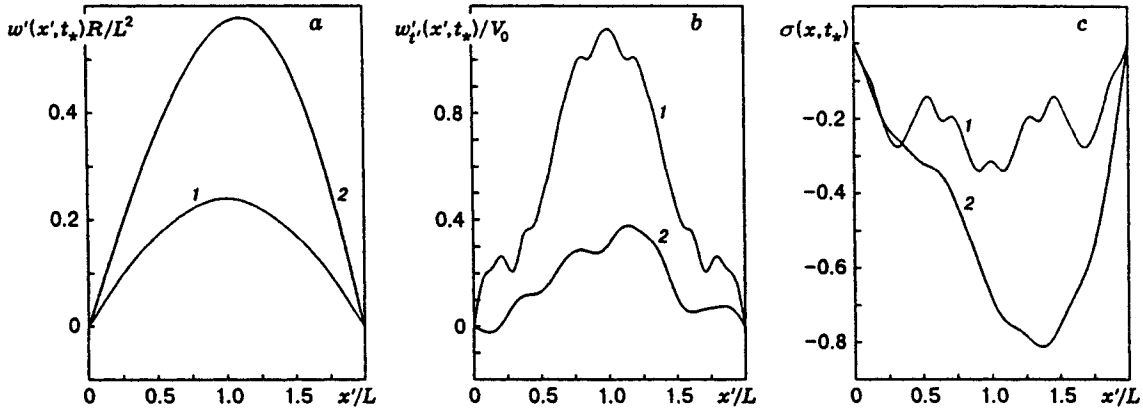

Fig. 4

in the contact region of the liquid and the elastic plate. We note that cavitational phenomena are not observed in the impact of undeformable plates.

It is natural to assume that the character of the interaction of an elastic plate with a liquid in the impact is basically determined by the dynamic rigidity of the plate β. The variation of the derivative $(dt/dc)(t)$ in time for $\beta = 0.02$ (curve 1) and $\beta = 0.06$ (curve 2) is plotted in Fig. 3b. The calculations were carried out for the first ten modes; as before, the parameter α equals 0.157. The transition from $\beta = 0.04$ to the case $\beta = 0.02$ means an increase of the impact velocity by a factor of $\sqrt{2}$, with other values being unchanged, and the transition to the case $\beta = 0.06$ means a decrease in the impact velocity by a factor $\sqrt{3/2}$. The impact conditions change slightly, but this leads to an abrupt change during the process. The increase in the impact velocity (curve 1) indicates the irregular character of the interaction of the elastic plate and the liquid. After half the plate is wetted, the contact spot begins to decrease. It goes beyond the framework of the assumptions of the problem, and the calculations must be stopped. As the impact velocity decreases (curve 2), the rate of wetting is limited and positive during the entire impact stage. For $\beta = 0.06$, the force that acts on the plate from the side of the liquid is bounded, but it can take negative values, as for $\beta = 0.04$.

Figure 4 compares the plate deflection (a), the velocity (b) of the plate points, and the distributions of the bending stresses in it (c) at the moment of completion of the impact stage in the case of a wave impact on the edge of the plate (curves 2) and in its center (curves 1). The impact conditions in both cases are identical, except the point of impact. Curves 1 are symmetric relative to the center of the plate ($x = 1$). The following values of the parameters were adopted in the calculations: $\alpha = 0.314$ and $\beta = 0.311$ [2]; this corresponds to the wave impact with a curvature radius at the wave crest of 10 m and a velocity of 3 m/sec on a plate made

from soft steel of thickness 2 cm and length 1 m. In dimensionless variables, the duration of the impact stage equals 0.36544 for the central impact and 1.53707 for the impact on the edge. It is seen that the growth of the duration of the impact stage causes a more than twofold increase in the deflection (Fig. 4a), the significant decrease in the kinetic energy of the beam (Fig. 4b), and the increase in the potential energy of the bending stresses (Fig. 4c). In the edge impact, the maximum stresses are reached at a distance of $0.6L$ from the right edge of the beam and are equal to 256 N/mm ^{2}. An analysis shows that the site of impact has a strong effect on the deformation of the plate at the end of the impact stage, with other conditions being equal.

This work was supported by the Russian Foundation for Fundamental Research (Grant No. 96-01-01767).

REFERENCES

1. A. A. Korobkin, "Wave impact on the bow end of a catamaran wet deck," *J. Ship Res.*, **39**, No. 4, 321–327 (1995).
2. A. A. Korobkin, "Wave impact on the center of an Euler beam," *Prikl. Mekh. Tekh. Fiz.*, **39**, No. 5, 134–147 (1998).
3. A. A. Korobkin, "Water impact problems in ship hydrodynamics," in: M. Ohkusu (ed.), *Advances in Marine Hydrodynamics*, Computational Mech. Publ., Southampton (1996), pp. 323–371.
4. M. Abramowitz and I. A. Stegun, *Handbook of Mathematical Functions with Formulas, Graphs, and Mathematical Tables*, John Wiley and Sons, New York (1972).
5. A. P. Prudnikov, Yu. A. Brychkov, and O. I. Marichev, *Integrals and Series, Mathematical Functions* [in Russian], Nauka, Moscow (1983).
6. A. A. Korobkin, "Acoustic approximation in the slamming problem," *J. Fluid Mech.*, **318**, 165–188 (1996).